THE BELL SYSTEM TECHNICAL JOURNAL
Vol. 56, No. 6, July–August 1977
Printed in U.S.A.

Reflection, Transmission, and Mode Conversion in a Corrugated Feed

By C. DRAGONE

(Manuscript received December 14, 1976)

Microwave antennas are often required to carry signals simultaneously over a broad range of frequencies—e.g., the combined TD-2 and TH common carrier bands encompass a total frequency ratio of about 1.8 to 1 as do the combined 18- and 30-GHz bands. To achieve these bandwidths, an efficient broadband feed horn is required. The corrugated (hybrid-mode) horn is a leading candidate, but it is not immune to some cross-polarization coupling, input reflection, and pattern asymmetry. These problems are introduced mainly by two phenomena: variation of the dominant mode shape with frequency and mode conversion along the horn taper and at waveguide transitions at the horn input. Simple formulas for computing the magnitude of these phenomena and their effects on return loss and radiation patterns are given.

I. INTRODUCTION

Corrugated feeds (also called hybrid-mode feeds) are widely used in reflector-type antennas because of their excellent radiation characteristics.[1-16] At the frequency ω_0 at which the surface reactance X_s of the corrugations becomes infinite, the radiation pattern of a properly designed feed is circularly symmetric, is free of cross-polarized components, and has low sidelobes. In principle these properties can be obtained over a frequency range of more than an octave. In fact, one can show that the

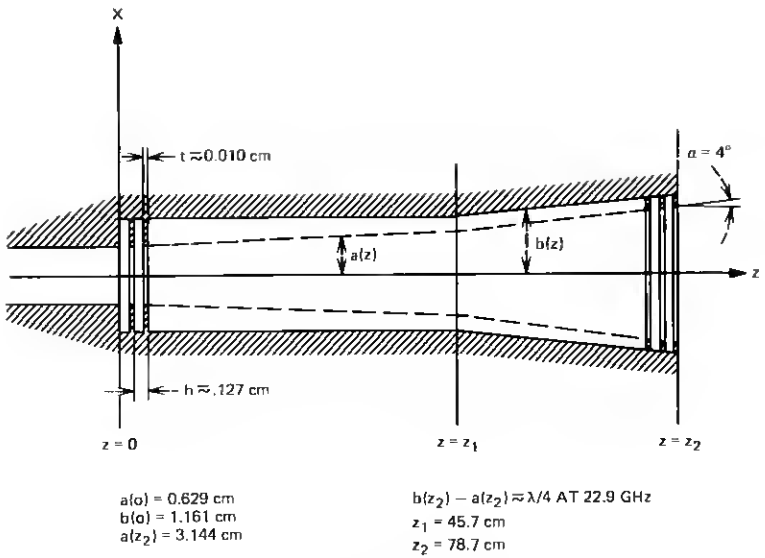

Fig. 1—Corrugated horn of Ref. 17.

field over an aperture illuminated by the fundamental mode has the remarkable property that in the limit, as

$$ka \to \infty, \quad (k = 2\pi/\lambda),$$

where a is the aperture radius, the field distribution becomes independent of the surface reactance X_s (provided $X_s \neq 0$). A corollary of this behavior is that a feed of sufficiently large aperture will have the above radiation characteristics over a wide range of frequencies provided only the fundamental mode is excited in the horn. To verify this behavior, an experiment, described in a companion article,[17] was made. A very long horn (see Fig. 1) was fabricated carefully, using a special fabrication technique to minimize geometrical imperfections in the corrugated walls, and the radiation characteristics were measured from 17 GHz to 35 GHz. From 17 GHz to 29 GHz the far field was found, as expected, to be essentially polarized in one direction. At frequencies above 29 GHz, however, a cross-polarized component was found to be caused by a certain undesirable mode, which will be called the HE'_{11}-mode. This mode was excited primarily at the input, where the corrugated waveguide was connected directly to a smooth waveguide, as shown in Fig. 1. A calculation, given in eqs. (102) and (103) of this article, was therefore made to determine the total amount of power converted from the TE_{11}-mode, incident at the input, to the HE'_{11}-mode.

A peculiarity of corrugated feeds is that there is some mode conversion even in a conical horn of constant surface reactance X_s (unless $X_s = 0$

or $X_s = \infty$). An evaluation of this effect is given in Section VII. However, in the experiment, the taper angle α (Fig. 1) was chosen sufficiently small ($\alpha \simeq 4°$) so that this effect was negligible.

The analysis starts in Section III with a derivation of the asymptotic properties for large ka of the modes of a corrugated waveguide. The results provide a simple and accurate representation of the modes in a feed aperture of more than a few wavelengths in diameter. Then, in Sections V and VI, a first-order derivation of the scattering parameters of a junction between two waveguides of slightly different characteristics is given. A simple relation [see, eqs. (83), (84), and (115) to (117)] is found between the scattering parameters and the coupling coefficients between the modes on the two sides of the junction. Each coefficient is given, except for a constant, by an integral of the type

$$\int\int_S (\mathbf{E}_1 \times \mathbf{H}_2^*) \cdot \mathbf{i}_z \, dxdy,$$

where S is the junction area, and $\mathbf{E}_1$ and $\mathbf{H}_2$ are the electric and magnetic vectors of the two modes, respectively. In Section IV, this surface integral is converted to a line integral, thus reducing the calculation of the coupling coefficients to a straightforward exercise. This result is useful also to calculate the far field of an aperture S illuminated by a mode $\mathbf{E}_1$, since the far field at a given observation point is, except for a constant, the coupling coefficient over S between $\mathbf{E}_1$ and the field $\mathbf{H}_2$ of a plane wave having the direction of the observation point. The far-field calculation is thus reduced to a contour integration.

The calculation of the scattering parameters is carried out in Sections IV to VI, using the above contour integral. It is found, for instance, that the input reflection of a corrugated feed connected to a smooth waveguide of the same diameter is simply given by the coefficient

$$\rho_1 = -\frac{\beta_1 - \beta_1'}{\beta_1 + \beta_1'},$$

β_1 and β_1' being the propagation constants in the two waveguides. An identical formula was derived by Brown[18] from the principle of conservation of momentum, but that derivation is not applicable to the present problem, which involves hybrid modes.

Finally, Section VII deals with the problem of spurious mode generation in a nonuniform waveguide whose parameters (radius and surface reactance) vary along the axis, as in Fig. 1. The differential scattering parameters that give, at any point in a nonuniform waveguide, the local coupling between the incident mode and the spurious modes are obtained from the analysis of Sections V and VI. By solving the differential equations specified by the above scattering parameters, we can thus determine the amplitudes of the spurious modes. An example is provided

of a first-order calculation of mode conversion in a conical waveguide such as the one in Fig. 1 for $z > z_1$. The result, eq. (154), is again quite simple.

II. PRELIMINARY CONSIDERATIONS

For a smooth waveguide, there is a simple relation between the propagation constant β of a mode and the waveguide diameter, but no such simple relation exists in the case of a corrugated waveguide [see eq. (20)]. For this reason, the properties of the corrugated waveguide modes cannot generally be determined as simply as in the case of a smooth waveguide. Also, the field configuration of each mode varies with waveguide diameter. There is, however, an important exception. When the radius a of the corrugated waveguide is sufficiently large, the propagation constant β for some of the modes is simply given by

$$\beta = \sqrt{(ka)^2 - u_{0m}^2}, \tag{1}$$

where u_{0m} is the mth zero of the Bessel function J_0 of order zero,

$$J_0(u_{0m}) = 0. \tag{2}$$

For all the other modes except one (for this special mode β is independent of a; see Appendix B) one has

$$\beta = \sqrt{(ka)^2 - u_{2m}^2}, \tag{3}$$

where u_{2m} is the mth root of the Bessel function of order two,

$$J_2(u_{2m}) = 0. \tag{4}$$

Equations (1) and (3) are valid provided $a \gg \lambda$, a condition which is satisfied to a good approximation by most feed apertures. Thus, the case

$$ka \gg 1 \tag{5}$$

is of considerable practical interest. One finds that as $ka \to \infty$, the properties of a mode become independent of the surface reactance X_s of the corrugated walls, except for the mode of Appendix B. Thus, the field distribution over the aperture of a feed illuminated by a single mode will be little affected by the surface reactance X_s (which varies fairly rapidly with frequency) provided ka is sufficiently large. This result, first pointed out by Thomas,[8] is very important for it implies that the aperture field distribution becomes frequency independent for large ka. The main purpose of this section is to determine the asymptotic behavior of the hybrid modes for large ka. It is shown that if $ka \neq \infty$ there is over the aperture of a feed a certain undesirable cross-polarized component, even if the aperture is illuminated by a single mode, unless of course X_s

$= \infty$. A simple expression for the amplitude of this component is given.

III. ASYMPTOTIC BEHAVIOR FOR LARGE *ka*

Consider a disk-loaded waveguide centered around the z-axis, as in Fig. 1, and assume its parameters a, b, and h are independent of z. Let r, ϕ, z be cylindrical coordinates defined by $x = r\cos\phi$ and $y = r\sin\phi$. The separation of the disks, which occupy the region $a < r < b$, is assumed to be much smaller than a wavelength λ,

$$kh \ll 1. \tag{6}$$

The region between two consecutive disks forms a radial line whose input reactance jX at $r = a$ is a function of the radial length $l = b - a$; for $ka \gg 1$, one has approximately

$$jX = jZ_0 \tan kl,$$

where $Z_0 = \sqrt{\mu_0/\epsilon_0}$. For a finite number of teeth per wavelength, the value of l must be corrected.* Because of condition (6) the effect of the disks can be accounted for adequately by introducing an effective surface reactance[5,12,19]

$$jX_s = jX\left(1 - \frac{t}{h}\right), \tag{7}$$

where t is the thickness of the disks, and by requiring that the field for $r < a$ satisfy the boundary conditions

$$\left.\begin{aligned} E_\phi &\simeq 0 \\ H_\phi &\simeq -\frac{E_z}{jX_s} \end{aligned}\right\} \text{for } r = a, \tag{8}$$

where E_ϕ, H_ϕ, E_z are the ϕ and z components of the electric and magnetic field.

Let β be the propagation constant in the z direction,

$$\beta = k\cos\theta_1, \tag{9}$$

and assume θ_1 is real, so that $\beta < k$. The case where θ_1 is imaginary is considered in Appendix B. Assume the ϕ dependence of E_z is given by $\cos\phi$. Then, the field components of a mode that propagates in the z direction with propagation constant β are eiven by

$$E_z = AJ_1(\kappa r)\cos\phi\, e^{-j\beta z}, \tag{10}$$

* See Ref. 17 for the effect of a finite number of teeth per wavelength, which causes a reduction of the effective depth, l.

$$Z_0 H_z = B J_1(\kappa r) \sin\phi \, e^{-j\beta z}, \tag{11}$$

$$E_\phi = \frac{j}{\sin\theta_1}\left[B J_1'(\kappa r) + A \cos\theta_1 \frac{J_1(\kappa r)}{\kappa r}\right] \sin\phi \, e^{-j\beta z}, \tag{12}$$

$$Z_0 H_\phi = -\frac{j}{\sin\theta_1}\left[A J_1'(\kappa r) + B \cos\theta_1 \frac{J_1(\kappa r)}{\kappa r}\right] \cos\phi \, e^{-j\beta z}, \tag{13}$$

$$E_\rho = -\frac{j}{\sin\theta_1}\left[B \frac{J_1(\kappa r)}{\kappa r} + A \cos\theta_1 J_1'(\kappa r)\right] \cos\phi \, e^{-j\beta z}, \tag{14}$$

$$Z_0 H_\rho = -\frac{j}{\sin\theta_1}\left[A \frac{J_1(\kappa r)}{\kappa r} + B \cos\theta_1 J_1'(\kappa r)\right] \sin\phi \, e^{-j\beta z}, \tag{15}$$

$$(r \leqq a),$$

where

$$\kappa = k \sin\theta_1.$$

The boundary conditions (8) give[12]

$$\gamma = -\frac{u}{\cos\theta_1} \frac{J_1'(u)}{J_1(u)}, \tag{16}$$

$$\mathrm{y} = \frac{\cos\theta_1}{\sin\theta_1} \frac{1}{u} \frac{1}{\gamma} + \frac{1}{\sin\theta_1} \frac{J_1'(u)}{J_1(u)}, \tag{17}$$

where

$$u = ka \sin\theta_1,$$

$$\mathrm{y} = -\frac{Z_0}{X_s}, \tag{18}$$

and γ is the ratio between the TM and TE components of the hybrid mode,

$$\gamma = \frac{A}{B}. \tag{19}$$

By eliminating γ from eqs. (16) and (17), one obtains the eigenvalue equation

$$\frac{\mathrm{y}}{ka} = \frac{1}{u^2} \frac{J_1(u)}{u J_1'(u)} \left[\left(\frac{u J_1'(u)}{J_1(u)} \right)^2 - 1 + \frac{u^2}{(ka)^2} \right], \tag{20}$$

which is eq. (10) of Ref. 12.

The solutions of this equation are now studied for large ka. Both u and y are assumed to be finite. Then, in the limit as $ka \to \infty$, eq. (20) reduces to

$$\left(\frac{J_1'(u)}{J_1(u)} u \right)^2 - 1 = 0. \tag{21}$$

We distinguish two cases:

$$\frac{J_1'(u)u}{J_1(u)} = -1 \tag{22}$$

and

$$\frac{J_1'(u)u}{J_1(u)} = 1. \tag{23}$$

According to eq. (16) (with $\cos\theta_1 \approx 1$, since $\theta_1 \to 0$ as $ka \to \infty$), these two cases correspond respectively to

$$\gamma = 1 \tag{24}$$

and

$$\gamma = -1. \tag{25}$$

Using well known recurrence relations between the Bessel functions and their derivatives, and using conditions (22) and (23), we find

$$J_0(u) = 0 \tag{26}$$

and

$$J_2(u) = 0. \tag{27}$$

We conclude that for large ka, eq. (20) possesses the two sets of solutions

$$u \approx u_{0m} \ (m = 1, 2, \text{etc.}) \tag{28}$$

and

$$u \approx u_{2m} \ (m = 1, 2, \text{etc.}), \tag{29}$$

u_{0m} and u_{2m} being respectively the mth root of $J_0(u)$ and $J_2(u)$. Solutions (28) and (29) are characterized by $\gamma \approx 1$ and $\gamma \approx -1$; the corresponding modes will be designated,* respectively, HE_{1m} and HE_{1m}'.

Asymptotic series for u and γ in terms of

$$\frac{1}{ka}, \tag{30}$$

* This mode classification differs from the one by Clarricoats[12] and it was chosen for the following reason. Here, and in Ref. 17, we are interested in horns whose inner radius a varies gradually with z, while the wall susceptance y is approximately constant, as in Fig. 1, from z_2 to z_1. Consider therefore a mode propagating in Fig. 1 from z_2 towards z_1. Clarricoats' classification assigns in some cases a different name to this mode in different regions of the horn, even though there will be no discontinuous variation of the mode-field configuration, as it propagates in the horn. On the other hand, our classification based on the Bessel function roots u_{0m} and u_{2m}, assigns a single name everywhere in the horn. If instead the frequency is gradually changed the mode of a waveguide of given dimensions will retain the same name with Clarricoats' classification, whereas this is not always true with our classification. To understand better these considerations, see also Ref. 25.

are derived in Appendix A under the assumption $y \neq \infty$. For the HE_{1m} modes, characterized by $\gamma \to 1$ as $ka \to \infty$, it is found that

$$u = u_m = u_{0m}\left\{1 - \frac{1}{2}\frac{y}{ka} - \frac{1}{2}\left[1 - \frac{y^2}{4}(1 + u_{0m}^2)\right]\left(\frac{1}{ka}\right)^2 + \frac{y}{4}\left[1 - \frac{y^2}{12}(7u_{0m}^2 + 1)\right]\left(\frac{1}{ka}\right)^3 \cdots\right\} \quad (31)$$

and

$$\gamma = 1 - u_{0m}^2\left\{\frac{y}{2}\frac{1}{ka} - \frac{y^2}{8}(4 + u_{0m}^2)\left(\frac{1}{ka}\right)^2 - \frac{y}{2}\left[1 - \frac{1}{2}u_{0m}^2 - \frac{y^2}{4}(3u_{0m}^2 + 2)\right]\left(\frac{1}{ka}\right)^3 \cdots\right\}. \quad (32)$$

For the HE'_{1m}-modes, characterized by $\gamma \to -1$, u is given by

$$u'_m = u_{2m}\left\{1 - \frac{1}{2}\frac{y}{ka} \cdots\right\} \quad (33)$$

and

$$\gamma = -1 - u_{2m}^2\left\{\frac{1}{2}\frac{y}{ka} \cdots\right\}. \quad (34)$$

The x and y components of the electric field are now derived. First consider the HE_{1m} modes. One finds from eqs. (10) to (15), with $\cos\theta_1 = 1$ and γ given by eq. (32), that for large ka the transverse component of $\mathbf{E}$ is given by

$$\mathbf{E}_t \approx -j\frac{ka}{u}A\left[J_0\left(\frac{r}{a}u\right)\mathbf{i}_x + \frac{1}{4}u^2\frac{y}{ka}J_2\left(\frac{r}{a}u\right)(\cos 2\phi\,\mathbf{i}_x + \sin 2\phi\,\mathbf{i}_y)\right], \quad (35)$$

omitting the factor $e^{-j\beta z}$. Amplitude A is determined by power P carried by the mode. From eq. (67) with du/dy given by eq. (92) and $\eta_i = A$

$$|A| \approx \frac{1}{a}\sqrt{\frac{Z_0}{\pi}\frac{1}{a\beta}\frac{u^2}{ka}\frac{1}{J_1^2(u)}} \quad (36)$$

if $P = \frac{1}{2}$.

For the HE'_{1m} modes with $\gamma \approx -1$, on the other hand,

$$\mathbf{E}_t \approx j\frac{ka}{u}A\left[J_2\left(\frac{r}{a}u\right)(\cos 2\phi\,\mathbf{i}_x + \sin 2\phi\,\mathbf{i}_y) + \cdots\right], \quad (37)$$

where the dots represent terms that vanish as $ka \to \infty$. The amplitude $|A|$ for $P = \frac{1}{2}$ is still given by eq. (36).*

An important property of the field distribution (35) is that $E_y \to 0$ as $ka \to \infty$. Thus, in the limit as $ka \to \infty$, the field becomes polarized in one direction, *regardless of the value of the surface reactance* X_s (unless, of course $X_s = 0$). From eq. (35), the amplitude of E_y is porportional to the ratio

$$\frac{y}{ka}. \tag{38}$$

Therefore, in order that E_y be negligible over the aperture of a feed, it is sufficient that the aperture diameter be large and the thickness t of the disks (see Fig. 1) be small compared with their separation.† The far field of an aperture illuminated by the fundamental mode, the HE_{11} mode given by eq. (35) for $u = u_{01} = 2.4048$, is discussed in Ref. 17. From a comparison of the radiation patterns of E_x and E_y, we find that the ratio C^2 between the maximum value attained by $|E_y|^2$ and $|E_x|^2$ (which occurs on axis) is given by

$$C^2 = 0.14 \left(\frac{y}{ka}\right)^2 = \frac{0.14}{\left[(1 - t/h)ka \tan \frac{\pi}{2} \frac{\omega}{\omega_0}\right]^2}, \tag{39}$$

where ω_0 denotes the frequency for which $y = 0$. One can easily verify using this formula that C^2 remains less than 0.000316 (−35 dB) over a frequency range $\omega_1 < \omega < 1.93\,\omega_1$, provided $ka > 10$ and $t/h < 0.1$.

Thus, good performance over a wide frequency range is possible, provided all the power incident at the input of the feed is converted to the HE_{11} mode. If, however, some of the input power is converted into some of the HE'_{1m} modes, then, according to eq. (37), the field over the feed aperture will contain a cross-polarized component whose amplitude is essentially independent of the ratio y/ka. The resulting cross-polarized component of the far field is discussed in Ref. 17. If $\omega_1 < \omega < \omega_2$ denotes the frequency range over which only the fundamental mode (HE_{11}) propagates, it is pointed out in Ref. 17 that the largest value that ω_2/ω_1 can assume is 1.6839; this value is attained for $b/a = 1.8309$. Cutoff frequency formulas are derived in Appendix D.

In Appendix B, the properties of a surface-wave mode that can exist in a corrugated waveguide, in addition to the modes of eqs. (35) and (37), are briefly described.

---

* In eqs. (35) and (37), only the leading terms for the symmetrical, asymmetrical, and cross-polarized components are retained.

† Note that from eqs. (7), (8), and (18), y increases with t/h.

IV. COUPLING COEFFICIENT BETWEEN TWO MODES

Suppose the electric field $\mathbf{E}_1$ at the input of a corrugated waveguide is known, and we want to determine the resulting amplitude of one of the modes excited in the corrugated waveguide. We have to evaluate a surface integral of the form

$$\int\int_S (\mathbf{E}_1 \times \mathbf{H}_2^*) \cdot \mathbf{i}_z \, dxdy, \tag{40}$$

where $\mathbf{H}_2$ is the magnetic field of the mode whose amplitude is to be determined. This integral, identical to that involved in determining the far field radiated in a given direction by an aperture containing the field $\mathbf{E}_1$, is in general difficult to evaluate. However, in many cases, we can assume that

$$\frac{\partial \mathbf{E}_1}{\partial z} \approx -j\beta_1 \mathbf{E}_1, \tag{41}$$

where β_1 is a constant. This condition is approximately satisfied,* for instance, in the case of a feed aperture illuminated by a single mode propagating in the z direction with propagation constant β_1. We will show that the above surface integral can be reduced to a line integral which can be evaluated straightforwardly. We use the symbol $(\mathbf{E}_1, \mathbf{H}_2)$ for the integral (40), and call it the scalar product of the two modes $\mathbf{E}_1$ and $\mathbf{H}_2$.

If $\mathbf{E}_1, \mathbf{H}_1$ and $\mathbf{E}_2, \mathbf{H}_2$ are two solutions of Maxwell's equations, in free space,[20]

$$\nabla \cdot (\mathbf{E}_1 \times \mathbf{H}_2^* + \mathbf{E}_2^* \times \mathbf{H}_1) = 0 \tag{42}$$

in the absence of sources. Now, let the z dependence of the two solutions be given by

$$e^{-j\beta_1 z} \quad \text{and} \quad e^{-j\beta_2 z}. \tag{43}$$

Then, in eq. (42)

$$\nabla = \nabla_t - j(\beta_1 - \beta_2)\mathbf{i}_z, \tag{44}$$

where ∇_t is the transverse part of ∇. Therefore eq. (42) gives

$$\nabla_t(\mathbf{E}_1 \times \mathbf{H}_2^* + \mathbf{E}_2^* \times \mathbf{H}_1) = j(\beta_1 - \beta_2)[(\mathbf{E}_1 \times \mathbf{H}_2^*) \cdot \mathbf{i}_z + (\mathbf{E}_2^* \times \mathbf{H}_1) \cdot \mathbf{i}_z]. \tag{45}$$

Next, consider a new solution $\mathbf{E}_1'$, $\mathbf{H}_1'$ with propagation constant $\beta_1' = -\beta_1$ and with z components given by

$$E_{1z}' = -E_{1z} \tag{46}$$

* Of course, condition (41) is satisfied *exactly* by a mode in a cylindrical waveguide.

$$H'_{1z} = +H_{1z}. \tag{47}$$

Then the x, y components of $\mathbf{E}'_1$, $\mathbf{H}'_1$ simply coincide[21] with the x, y components of $\mathbf{E}_1$, $-\mathbf{H}_1$,

$$E'_{1x} = E_{1x}, \qquad E'_{1y} = E_{1y}, \tag{48}$$

$$H'_{1x} = -H_{1x}, \qquad H'_{1y} = -H_{1y}. \tag{49}$$

Therefore, replacing in eq. (45) β_1, $\mathbf{E}_1$, $\mathbf{H}_1$ with $-\beta_1$, $\mathbf{E}'_1$, $\mathbf{H}'_1$ and making use of eqs. (48) and (49), we obtain

$$\nabla_t \cdot (\mathbf{E}'_1 \times \mathbf{H}^*_2 + \mathbf{E}^*_2 \times \mathbf{H}'_1) = -j(\beta_1 + \beta_2)[(\mathbf{E}_1 \times \mathbf{H}^*_2) - (\mathbf{E}^*_2 \cdot \mathbf{H}_1)] \times \mathbf{i}_z. \tag{50}$$

By adding eq. (45) to eq. (50), we obtain

$$(\mathbf{E}_1 \times \mathbf{H}^*_2) \cdot \mathbf{i}_z = \nabla_t \cdot \mathbf{F}, \tag{51}$$

where

$$\mathbf{F} = \frac{j}{2(\beta_1 + \beta_2)} [\mathbf{E}'_1 \times \mathbf{H}^*_2 + \mathbf{E}^*_2 \times \mathbf{H}'_1] - \frac{j}{2(\beta_1 - \beta_2)} [(\mathbf{E}_1 \times \mathbf{H}^*_2) + (\mathbf{E}^*_2 \times \mathbf{H}_1)]. \tag{52}$$

We now integrate eq. (51) over a finite area S of the plane $z = 0$, making use of the divergence theorem,

$$\int\int_S (\mathbf{E}_1 \times \mathbf{H}^*_2) \cdot \mathbf{i}_z \, dxdy = \oint_C \mathbf{F} \cdot \mathbf{n} \, ds, \tag{53}$$

where C is the contour of S and $\mathbf{n}$ is the outward normal. To determine $\mathbf{F} \cdot \mathbf{n}$, let τ be a unit vector tangent to C,

$$\tau = \mathbf{i}_z \times \mathbf{n}. \tag{54}$$

Then, if $\mathbf{A}$ and $\mathbf{B}$ are two arbitrary vectors,

$$(\mathbf{A} \times \mathbf{B}) \cdot \mathbf{n} = A_\tau B_z - A_z B_\tau, \tag{55}$$

where A_τ, B_τ are the components of $\mathbf{A}$ and $\mathbf{B}$ in the direction of τ. Therefore, from eq. (52), taking into account eqs. (46) to (49),

$$\mathbf{F} \cdot \mathbf{n} = -j \frac{\beta_2}{\beta_1^2 - \beta_2^2} [E_{1\tau} H^*_{2z} + E^*_{2\tau} H_{1z}] + j \frac{\beta_1}{\beta_1^2 - \beta_2^2} [E_{1z} H^*_{2\tau} + E^*_{2z} H_{1\tau}]. \tag{56}$$

Finally, from eqs. (53) and (56), we obtain the desired result,

$$(\mathbf{E}_1, \mathbf{H}_2) = \int\int_S (\mathbf{E}_1 \times \mathbf{H}_2^*) \cdot \mathbf{i}_z \, dxdy$$

$$= -j \frac{\beta_2}{\beta_1^2 - \beta_2^2} \oint_C (E_{1\tau} H_{2z}^* + E_{2\tau}^* H_{1z}) ds$$

$$+ j \frac{\beta_1}{\beta_1^2 - \beta_2^2} \oint_C (E_{1z} H_{2\tau}^* + E_{2z}^* H_{1\tau}) ds. \quad (57)$$

Thus, the scalar product (coupling coefficient) of two modes $\mathbf{E}_1$ and $\mathbf{E}_2$ can be determined straightforwardly from the values of $\mathbf{E}_1$ and $\mathbf{E}_2$ on the contour of the aperture S. This result has a number of applications. It can be used, as already pointed out, to determine the far field radiated by an aperture S with known field distribution $\mathbf{E}_1$, in which case $\mathbf{H}_2$ is the magnetic field* of a plane wave with propagation vector $\mathbf{k}$ and eq. (57) gives, except for a constant independent of $\mathbf{k}$, the field component radiated in the direction of $\mathbf{k}$ with the polarization of $\mathbf{H}_2$. In this article, we are interested in the special case where S is a circular area of radius a, in which case we can replace in eq. (57) τ with ϕ, since

$$\tau = \mathbf{i}_\phi.$$

If $\mathbf{E}_i$, $\mathbf{H}_i$ $(i = 1, 2)$ represents a mode of a corrugated waveguide of radius a, so that for $r = a$

$$E_{i\phi} = 0, \quad Z_0 H_{i\phi} = -j\mathrm{y}_i E_{iz}, \quad (58)$$

then eq. (57) simplifies to

$$(\mathbf{E}_1, \mathbf{H}_2) = -\frac{1}{Z_0} \frac{\beta_1}{\beta_1^2 - \beta_2^2} (\mathrm{y}_2 - \mathrm{y}_1) \oint_C E_{1z} E_{2z}^* \, ds. \quad (59)$$

Since the modes are characterized for $z = 0$ and $r = a$ by

$$E_{iz} = \eta_i J_1(u_i) \cos\phi, \quad (60)$$

where η_i is the coefficient A of the ith mode, then

$$(\mathbf{E}_1, \mathbf{H}_2) = -\frac{a\pi}{Z_0} \frac{\beta_1}{\beta_1^2 - \beta_2^2} (\mathrm{y}_2 - \mathrm{y}_1) \eta_1 \eta_2^* J_1(u_1) J_1(u_2). \quad (61)$$

Note that

$$a^2(\beta_1^2 - \beta_2^2) = u_2^2 - u_1^2. \quad (62)$$

If we assume

$$\mathrm{y}_2 = \mathrm{y}_1 + d\mathrm{y}, \quad (63)$$

$$u_2 = u_1 + du_1, \quad (64)$$

* There are two cases (two polarizations) that must be considered, for each value of $\mathbf{k}$.

from eq. (61) we obtain for the power carried by the mode $\mathbf{E}_1$

$$P_1 = \frac{1}{2}(\mathbf{E}_1, \mathbf{H}_1) = -\frac{\pi}{2Z_0}\frac{\beta_1 a^3}{2u_1}\frac{dy}{du_1}\eta_1^2 J_1^2(u_1). \tag{65}$$

The derivative dy/du_1, which appears in this expression, is calculated in Appendix C. In the following sections, we choose

$$(\mathbf{E}_i, \mathbf{H}_i) = 1, \tag{66}$$

in which case from eq. (65)

$$|\eta_i| = \sqrt{\frac{2Z_0}{a^2\pi}\frac{u_i}{\beta_i a}\left|\frac{du_i}{dy}\right|\frac{1}{J_1^2(u_i)}}. \tag{67}$$

These results are now applied to the problem of a junction between two different waveguides.

V. JUNCTION BETWEEN TWO WAVEGUIDES OF DIFFERENT SURFACE REACTANCE

Let two waveguides of different surface reactance, but the same diameter, be jointed at $z = 0$. Assume a single mode incident on the plane of the junction from the region $z < 0$ and let $\mathbf{E}_t$, $\mathbf{H}_t$ denote the transverse field components. To determine the amplitudes of the reflected and transmitted modes, we expand $\mathbf{E}_t$ and $\mathbf{H}_t$ on either side of the junction in an infinite series of modes, and then require continuity of $\mathbf{E}_t$ and $\mathbf{H}_t$ at the junction. A simple solution for the amplitudes of the scattered modes is then obtained assuming the difference in surface reactance is small. This result will be extended in Section VI to the more general case of two waveguides of slightly different diameter.

Let the transverse fields for $z < 0$ be represented by a superposition of the modes of the waveguide occupying the region $z < 0$,

$$\mathbf{E}_t = A_1\mathbf{e}_1 e^{-j\beta_1 z} + \sum_1^\infty R_i\mathbf{e}_i e^{j\beta_1 z}, \quad (z < 0) \tag{68}$$

$$\mathbf{H}_t = A_1\mathbf{h}_1 e^{-j\beta_1 z} - \sum_1^\infty R_i\mathbf{h}_i e^{j\beta_1 z}, \quad (z < 0), \tag{69}$$

where

$$A_1\mathbf{e}_1 e^{-j\beta_1 z}, \quad A_1\mathbf{h}_1 e^{-j\beta_1 z} \quad (\mathrm{Re}(\beta_1) > 0)$$

are the transverse field components of the incident mode, and

$$R_i\mathbf{e}_i e^{j\beta_i z}, \quad -R_i\mathbf{h}_i e^{j\beta_i z}$$

are those of the reflected modes.

Similarly, for $z > 0$,

$$\mathbf{E}_t = \sum_1^\infty T_i \mathbf{e}_i' e^{-j\beta_i' z}, \quad (z > 0) \tag{70}$$

$$\mathbf{H}_t = \sum_1^\infty T_i \mathbf{h}_i' e^{-j\beta_i' z}, \quad (z > 0), \tag{71}$$

where T_i are the amplitudes of the transmitted modes.

We assume that $\mathbf{e}_i$, $\mathbf{h}_i$ are normalized so that

$$(\mathbf{e}_i, \mathbf{h}_n) = \int\int_S (\mathbf{e}_1 \times \mathbf{h}_n^*) \cdot i_z \quad dxdy = \delta_{in}. \tag{72}$$

Similarly,

$$(\mathbf{e}_i', \mathbf{h}_n') = \delta_{in}. \tag{73}$$

Since $(\mathbf{e}_i, \mathbf{h}_i)$ represents twice the power carried by the ith mode $\mathbf{e}_i$, this power becomes imaginary if the mode is cutoff, in which case eq. (73) for $i = 1$ should be replaced with

$$(\mathbf{e}_i, \mathbf{h}_i) = j.$$

However, in this article the calculation of R_i, T_i is restricted to the modes that are not cut off by the two waveguides.

From eq. (61) with η_i, η_k given by eq. (67),

$$(\mathbf{e}_i, \mathbf{h}_n') = \frac{2}{a^2} \frac{\beta_i}{\beta_i^2 - \beta_n'^2} (\mathrm{y} - \mathrm{y}') \sqrt{\frac{u_i u_n'}{|\beta_i \beta_n' (d\mathrm{y}/du_i)(d\mathrm{y}'/du_n')|}}. \tag{74}$$

and

$$(\mathbf{e}_n', \mathbf{h}_i) = \frac{\beta_n'}{\beta_i} (\mathbf{e}_i, \mathbf{h}_n'), \tag{75}$$

where $(\mathbf{e}_i, \mathbf{h}_n')$ and $(\mathbf{e}_n', \mathbf{h}_i)$ are scalar products defined as in eq. (72) and

$$u_i^2 = (ka)^2 - (\beta_i a)^2, \tag{76}$$

a being the radius of the two waveguides. In eq. (74) 1/y and 1/y′ are the normalized surface reactances of the two waveguides.

Now assume $\mathrm{y}' - \mathrm{y}$ is very small and let

$$\delta\mathrm{y} = \mathrm{y}' - \mathrm{y}. \tag{77}$$

To determine R_i, T_i, we require continuity of $\mathbf{E}_t$ and $\mathbf{H}_t$ for $z = 0$,

$$A_1 \mathbf{e}_1 + \sum_1^\infty R_n \mathbf{e}_n = T_1 \mathbf{e}_1' + \sum_2^\infty T_n \mathbf{e}_n'. \tag{78}$$

$$A_1 \mathbf{h}_1 - \sum_1^\infty R_n \mathbf{h}_n = T_1 \mathbf{h}_1' + \sum_2^\infty T_n \mathbf{h}_n'. \tag{79}$$

Take the scalar product of the first equation with $\mathbf{h}_i'$ and of the second with $\mathbf{e}_i'$. One obtains, taking into account eq. (73) and assuming that the mode $\mathbf{e}_i'$ is not cutoff, so that β_i' is real,

$$A_1(\mathbf{e}_1, \mathbf{h}_i') + R_i(\mathbf{e}_i, \mathbf{h}_i') + \sum_{n \neq 1,i} R_n(\mathbf{e}_n, \mathbf{h}_i') = T_i, \tag{80}$$

$$A_1(\mathbf{e}_i', \mathbf{h}_1) - R_i(\mathbf{e}_i', \mathbf{h}_i) - \sum_{n \neq 1,i} R_n(\mathbf{e}_i', \mathbf{h}_n) = T_i. \tag{81}$$

Now, assume for the moment that $y, y' \neq \infty$. Furthermore assume *none of the modes under consideration is at cutoff. Then*

$$(\mathbf{e}_n, \mathbf{h}_1'), \quad (\mathbf{e}_i', h_n) \quad (i \neq n) \tag{82}$$

are small quantities of the same order of δy. Furthermore, as we show below, this is true also for R_n. It follows that the two sums involving R_n in eqs. (80) and (81) are of order higher than δy. Therefore, subtracting these two equations and neglecting terms of order higher than δy,

$$R_i = -A_1 \frac{(\mathbf{e}_1, \mathbf{h}_i') - (\mathbf{e}_i', \mathbf{h}_1)}{(\mathbf{e}_i, \mathbf{h}_i') + (\mathbf{e}_i', \mathbf{h}_i)}. \tag{83}$$

Adding eqs. (80) and (81), and neglecting terms of order higher than δy and solving for T_i, we obtain

$$T_i = A_1 \frac{(\mathbf{e}_1, \mathbf{h}_i') + (\mathbf{e}_i', \mathbf{h}_1)}{2}. \tag{84}$$

Using eqs. (74) and (75), we rewrite eqs. (83) and (84) in the form

$$R_i = -A_1 \frac{\beta_i - \beta_i'}{\beta_1 + \beta_i'} \sqrt{\frac{u_1 \beta_i}{u_i \beta_1}} \sqrt{\left| \frac{dy/du_i}{dy/du_1} \right|}, \tag{85}$$

$$T_i = A_1 \frac{1}{a^2} \frac{1}{\beta_1 - \beta_i'} (y - y') \sqrt{\frac{u_1 u_i'}{\beta_1 \beta_i'}} \frac{1}{|(dy/du_1)\,(dy'/du_i')|}. \tag{86}$$

The derivatives dy/du_1 and dy'/du_i' are derived in Appendix C.

It is interesting to note from eq. (85) that the reflection coefficient for the mode $i = 1$ is simply

$$\rho_1 = \frac{R_1}{A_1} = -\frac{\beta_1 - \beta_1'}{\beta_1 + \beta_1'}, \tag{87}$$

which coincides with a formula derived by Brown[18] from a principle of conservation of momentum. However, that derivation is not applicable to the present problem, which involves hybrid modes. Measurements of ρ_1 described in Ref. 17 show that this formula, although derived assuming $y' \approx y$, is quite accurate even for relatively large differences between y and y'.

It is also interesting to note that the following interpretation can be given to eq. (86). If $\mathbf{E}_t$ for $z = 0$ were known, we could determine T_i simply using the formula

$$T_i = (\mathbf{E}_t, \mathbf{h}_i'), \quad (z = 0), \tag{88}$$

which follows from eq. (70), in view of the orthogonality relations (73). Now, if $y - y' \approx 0$, $\mathbf{E}_t$ does not differ much from $A_1\mathbf{e}_1$ and, therefore, we might be tempted to write in eq. (88) $\mathbf{E}_t \approx A_1\mathbf{e}_1$, in which case we would get

$$T_i \approx A_1(\mathbf{e}_1, \mathbf{h}_i'). \tag{89}$$

Alternatively, since from eq. (71) we also have

$$T_i = (\mathbf{e}_i', \mathbf{H}_t) \quad \text{for } z = 0, \tag{90}$$

we might be tempted to assume $\mathbf{H}_t \approx A_1\mathbf{h}_1$ for $z = 0$, in which case

$$T_i \approx A_1(\mathbf{e}_i', \mathbf{h}_1). \tag{91}$$

Neither of the two formulas is correct* even if $\delta y \approx 0$. However, according to eq. (84), a correct expression for small δy is obtained by taking the average of the two formulas. We now treat two special cases.

5.1 Limiting case ka ≫ 1

Assume that both y and y′ are finite, but the radius a is very large,

$$ka \gg 1,$$

a condition which is often satisfied near the aperture of a feed. From eqs. (31) and (33)

$$\lim_{ka\to\infty} \frac{du}{dy} = -\frac{1}{2}\frac{u}{ka}. \tag{92}$$

Furthermore, for large ka,

$$\beta a \approx ka - \frac{1}{2}\frac{u^2}{ka}, \tag{93}$$

since $(\beta a)^2 = (ka)^2 - u^2$. Therefore,

$$a\beta_i' - a\beta_i \approx -\frac{1}{2}\frac{u_i'^2 - u_i^2}{ka} \approx \frac{1}{2}\left(\frac{u_i}{ka}\right)^2 \delta y, \tag{94}$$

since from eq. (92)

$$u_i' \approx u_i - \frac{1}{2}\frac{u}{ka}\,\delta y. \tag{95}$$

* They are often used, however.[22]

Using these results, from eqs. (85) and (86) we obtain

$$T_i = -A_1 \frac{u_1 u_i}{u_i^2 - u_1^2} \frac{(y' - y)}{ka}, \tag{96}$$

$$R_i = A_1 \frac{1}{4} \frac{u_i u_1}{(ka)^2} \frac{y' - y}{ka}. \tag{97}$$

One can show that these formulas are valid even if δy is not small, provided both

$$\frac{y'}{ka} \quad \text{and} \quad \frac{y}{ka}$$

are small.

An application of eq. (96) is considered in Section 7.1.

5.2 Case 1/y = 0

At the input of the feed of Fig. 1, the corrugated waveguide is connected to a smooth waveguide ($1/y = 0$) of the same diameter. We now wish to calculate the reflection and transmission coefficients of such a junction. Thus, assume $y \eqsim \infty$ for $z < 0$. For $y \eqsim \infty$, there are two types of modes: TE modes, in which case $\gamma \eqsim 0$, and TM modes, in which case $\gamma \eqsim \infty$. In the former case, from eq. (179) of Appendix C

$$\lim_{y \to \infty} \frac{dy}{du} = -y^2(u^2 - 1) \frac{kau}{(ka)^2 - u^2}, \quad (\gamma \eqsim 0). \tag{98}$$

In the latter case, from eq. (180)

$$\frac{dy}{du} \eqsim -\frac{u}{ka} y^2 \quad (\gamma \eqsim \infty). \tag{99}$$

Now let the incident mode be a TE_{11} mode. We distinguish two cases depending on whether the ith mode is a TM mode or a TE mode. In the former case, from eqs. (85) and (98)

$$\lim_{y \to \infty} R_i = -A_1 \frac{\beta_i - \beta_i'}{\beta_1 + \beta_i'} \sqrt{\frac{\beta_i \beta_1}{(u_1^2 - 1)}} \frac{1}{k}, \tag{100}$$

where u_1 is the first root of $J_1'(u_1) = 0$,

$$u_1 = 1.8411. \tag{101}$$

If, on the other hand, the ith mode is also a TE-mode, from eqs. (85) and (99),

$$\lim_{y \to \infty} R_i = -A_i \frac{\beta_i - \beta_i'}{\beta_1 + \beta_i'} \sqrt{\frac{\beta_1}{\beta_i} \frac{u_i^2 - 1}{u_1^2 - 1}}. \tag{102}$$

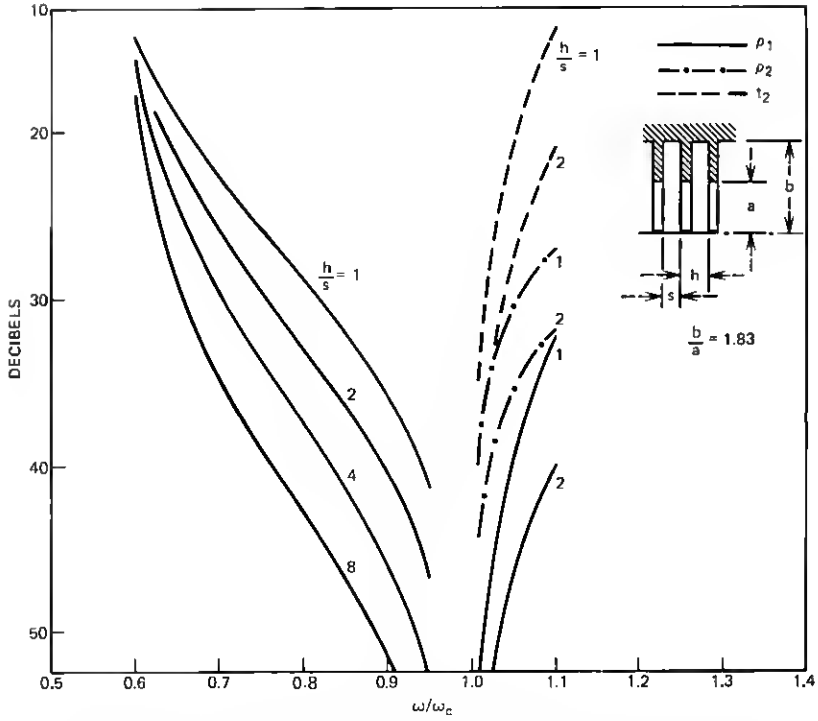

Fig. 2—Reflection, transmission, and coupling coefficients for input junction of Fig. 1.

From eq. (86) we obtain, using eq. (98),

$$\lim_{y\to\infty} T_i = A_1 \frac{1}{a\beta_1 - a\beta_i'} \sqrt{\frac{\beta_1 u_i'}{ka\beta_i'(u_1^2 - 1)}} \frac{1}{\sqrt{\left|\frac{dy'}{du_i'}\right|}}, \tag{103}$$

where dy'/du_i' can be determined using eq. (178), unless $y' \gg 1$, in which case we can use eq. (98) or (99) with y,u replaced by y', u_i'.

Equations (100) to (103) have been used to calculate the behavior of a junction with $b = 1.8309a$. Consideration has been restricted to the TE_{11} mode and the TM_{11} mode of the smooth waveguide, and the corresponding modes (HE_{11} and HE_{11}') of the corrugated waveguide. The results are shown in Fig. 2, where $i = 2$ refers to the TM_{11} mode (or the HE_{11}' mode),

$$\rho_1^2 = \left|\frac{R_1}{A_1}\right|^2 \tag{104}$$

is the input reflection,

$$\rho_2^2 = \left|\frac{R_2}{A_1}\right|^2 \tag{105}$$

gives the power converted into the TM_{11} mode, and

$$t_2^2 = \left|\frac{T_2}{A_1}\right|^2 \tag{106}$$

gives the power converted into the HE'_{11} mode. In Fig. 2, ω_c is the frequency at which $y' = \infty$. The corrugated guide at this frequency behaves like a smooth guide and, hence,

$$\rho_1 = \rho_2 = t_2 = 0. \tag{107}$$

The curves of Fig. 2 are useful in determining the practical bandwidth of the junction of Fig. 1.

VI. JUNCTION BETWEEN TWO WAVEGUIDES OF DIFFERENT DIAMETER

For some applications, to minimize the input reflection of a corrugated feed, it may be convenient to choose for the smooth waveguide a diameter different from that of the corrugated waveguide. In this section, the analysis of Section V is extended to the general case of a junction between two corrugated waveguides of different diameter. Let a and a' be the two diameters for $z > 0$ and $z < 0$, respectively, and assume again a single mode is incident on the junction, from the region $z < 0$.

If $\mathbf{E}_t$ for $z = 0$ were known, then the transmission coefficients T_i which appear in eqs. (70) and (71) could be determined at once using the formula*

$$T_i = \int\int_{S'} (\mathbf{E}_t \times \mathbf{h}_i^*) \cdot \mathbf{i}_z \, dS, \quad \text{for } z = 0, \tag{108}$$

which follows directly from eq. (70) in view of the orthogonality of the modes $\mathbf{e}'_i$, $\mathbf{h}'_i$ [see eq. (73)]. In eq. (108) S' denotes the circular area

$$0 < r < a'.$$

Now, for $z = 0$, $\mathbf{E}_t$ is given by eq. (68) inside the area

$$0 < r < a, \tag{109}$$

and it vanishes for $a < r < a'$. Therefore, eqs. (108) and (68) give

$$T_i = A_1(\mathbf{e}_1, \mathbf{h}'_i) + \sum_{n=1}^{\infty} R_n(\mathbf{e}_n, \mathbf{h}'_i), \tag{110}$$

where

$$(\mathbf{e}_n, \mathbf{h}'_i) = \int\int_S (\mathbf{e}_n \times \mathbf{h}'^*_i) \cdot \mathbf{i}_z \, dS, \tag{111}$$

S being the circular area (109), which corresponds to the waveguide of the region $z < 0$.

* Here we are only interested in calculating T_i and R_i for $\beta_i > 0$, $\beta'_i > 0$.

Equation (79), which was obtained by requiring continuity of $\mathbf{H}_t$ for $z = 0$, must be satisfied over the area S. By multiplying this equation with $\mathbf{e}_n$ and integrating over S, we obtain for $n \neq 1$

$$-R_n = \sum_1^\infty T_i(\mathbf{e}_n, \mathbf{h}_i') \quad (n \neq 1). \tag{112}$$

If the coefficients T_i in this relation are expressed in terms of the coefficients R_i using eq. (110), we get for $n \neq 1$

$$-R_n = (A_1 + R_1) \sum_{i=1}^{\infty} (\mathbf{e}_1, \mathbf{h}_i')(\mathbf{e}_n, \mathbf{h}_i') + R_n \sum_{i=1}^{\infty} (\mathbf{e}_n, \mathbf{h}_i')^2 + \sum_{s \neq n,1} R_s \sum_{i=1}^{\infty} (\mathbf{e}_s, \mathbf{h}_i')(\mathbf{e}_n, \mathbf{h}_i'). \tag{113}$$

For $n = 1$, the second sum of the right-hand side should be omitted and, furthermore, $-R_n$ should be replaced with $A_1 - R_1$.

We have thus obtained a system of equations in the unknowns R_1, R_2, etc. We solve* them in the limiting case where both $a' - a$ and $y' - y$ are very small, in which case

$$\left.\begin{aligned} (\mathbf{e}_n, \mathbf{h}_s') &\simeq 0 \quad \text{for } n \neq s \\ R_i &\simeq 0 \\ (\mathbf{e}_n, \mathbf{h}_k') - 1 &\simeq 0 \end{aligned}\right\}, \tag{114}$$

and therefore the first two terms of the right-hand side of eq. (113) for $n \neq 1$ are respectively equal to

$$A_1[(\mathbf{e}_n, \mathbf{h}_1') + (\mathbf{e}_1, \mathbf{h}_n')]$$

and R_n. The last term can be neglected. Therefore, eq. (113) gives for $n \neq 1$

$$R_n \simeq -\frac{1}{2}[(\mathbf{e}_1, \mathbf{h}_n') + (\mathbf{e}_n, \mathbf{h}_1')]A_1 \quad (n \neq 1). \tag{115}$$

Similarly, for $n = 1$,

$$R_1 \simeq \frac{1}{2}[1 - (\mathbf{e}_1, \mathbf{h}_1')^2]A_1 \simeq [1 - (\mathbf{e}_1, \mathbf{h}_1')]A_1. \tag{116}$$

The transmission coefficients can now be determined using eq. (110). We find for $n \neq 1$

$$T_n \simeq \frac{1}{2}[(\mathbf{e}_1, \mathbf{h}_n') - (\mathbf{e}_n, \mathbf{h}_1')]A_1, \quad (n \neq 1), \tag{117}$$

which is a generalization of eq. (84).

* This derivation is not rigorous, for we neglect to examine the question of convergence of the summations in eq. (113). However, the validity of the results appears to be confirmed by the experimental results.

The coefficients $(\mathbf{e}_i, \mathbf{h}_n')$ can be calculated using eq. (57). If $y' - y$ and $a' - a$ are very small, we can proceed as follows. The field components $\mathbf{e}_n$ and $\mathbf{h}_n$ of the nth mode are considered to be functions of the coordinates r,ϕ and of the two waveguide parameters a,y. Therefore,

$$\mathbf{h}_n' = \mathbf{h}_n(r, \phi, a', y') \simeq \mathbf{h}_n + \frac{\partial \mathbf{h}_n}{\partial y}\delta y + \frac{\partial \mathbf{h}_n}{\partial a}\delta a, \tag{118}$$

where $\mathbf{h}_n$, $\partial \mathbf{h}_n/\partial y$ and $\partial \mathbf{h}_n/\partial a$ are evaluated for $a' = a$, $y' = y$, and δy are δa denote $y' - y$ and $a' - a$. a similar relation can be written for $\mathbf{e}_n'$. It follows from eq. (118) that $(\mathbf{e}_i, \mathbf{h}_n')$ for $i \neq n$ is a sum of two terms,

$$(\mathbf{e}_i, \mathbf{h}_n') = \left(\mathbf{e}_i, \frac{\partial \mathbf{h}_n}{\partial y}\right)\delta y + \left(\mathbf{e}_i \frac{\partial \mathbf{h}_n}{\partial a}\right)\delta a, \tag{119}$$

since $(\mathbf{e}_i, \mathbf{h}_n) = 0$. The first term is simply the coefficient $(\mathbf{e}_i, \mathbf{h}_n')$ calculated for $a' = a$; it corresponds to a junction between two waveguides of the same radius, but different surface reactance. The second term can be interpreted as the coefficient $(\mathbf{e}_i, \mathbf{h}_n')$ relative to a junction between two waveguides having the same surface reactance but different radii a and a'. Since the term has already been treated in Section V, only the latter need be considered. If one sets

$$\delta \mathbf{h}_n = \frac{\partial \mathbf{h}_n}{\partial a}\delta a, \quad \delta \mathbf{e}_n = \frac{\partial \mathbf{e}_n}{\partial a}\delta a, \tag{120}$$

and if the ϕ variations of both modes are of the type considered in Section I, then, taking into account that $e_{i\phi} = 0$ for $r = a$, using eq. (57) we get

$$(\mathbf{e}_i, \delta \mathbf{h}_n) = \pi a \delta a \left[-j \frac{\beta_n}{\beta_i^2 - \beta_n^2} \left(e_{i\phi} \frac{\partial h_{nz}^*}{\partial a} + \frac{\partial e_{n\phi}^*}{\partial a} h_{iz} \right)_{\substack{\phi=90^\circ \\ r=a}} \right.$$
$$\left. + j \frac{\beta_i}{\beta_i^2 - \beta_n^2} \left(e_{iz} \frac{\partial h_{n\phi}^*}{\partial a} + \frac{\partial e_{nz}^*}{\partial a} h_{i\phi} \right)_{\substack{\phi=0^\circ \\ r=a}} \right]. \tag{121}$$

As an application, consider $y = \infty$, in which case $(\mathbf{e}_i, \mathbf{h}_n')$ can be interpreted as the coefficient $(\mathbf{e}_i, \mathbf{h}_n')$ relative to a junction between two smooth waveguides of radii a and $a' = a + \delta a$, respectively. Assume $\mathbf{e}_i$ is a TE mode and $\mathbf{e}_n$ is a TM mode, so that for $r = a$

$$e_{i\phi} = e_{iz} = \frac{\partial h_{nz}^*}{\partial a} = 0, \tag{122}$$

where the last term vanishes because $\mathbf{h}_n$ is a TM mode. Then eq. (121) gives

$$(\mathbf{e}_i, \delta \mathbf{h}_n) = \pi a \delta a \frac{1}{\beta_i^2 - \beta_n^2} \left[-j\beta_n \left(\frac{\partial e_{n\phi}^*}{\partial a} h_{iz} \right)_{\substack{\phi=90^\circ \\ r=a}} \right.$$
$$\left. + j\beta_i \left(\frac{\partial e_{nz}^*}{\partial a} h_{i\phi} \right)_{\substack{\phi=0^\circ \\ r=a}} \right]. \tag{123}$$

Similarly, interchanging $n \leftrightarrows i$ in eq. (121) and taking into account that for $r = a$

$$\frac{\partial e_{iz}}{\partial a} = e_{n\phi} = e_{nz} = h_{nz} = 0, \tag{124}$$

we obtain

$$(\mathbf{e}_n, \delta \mathbf{h}_i) = 0. \tag{125}$$

Now, the two modes are characterized by

$$h_{iz} = \frac{1}{Z_0} \eta_i J_1 \left(\frac{r}{a} u_i\right) \sin\phi, \tag{126}$$

$$h_{i\phi} = -\frac{j}{Z_0} \eta_i \frac{\beta_i a}{u_i} \frac{J_1 \left(\frac{r}{a} u_i\right)}{\frac{r}{a} u_i} \cos\phi, \tag{127}$$

and

$$e_{nz} = \eta_n J_1 \left(\frac{r}{a} u_n\right) \cos\phi, \tag{128}$$

$$e_{n\phi} = j\eta_n \frac{\beta_n a}{u_n} \frac{J_1 \left(\frac{r}{a} u_n\right)}{\frac{r}{a} u_n} \sin\phi, \tag{129}$$

where the amplitudes η_i and η_n are, because of the requirement (72), given by

$$\eta_i = \sqrt{\frac{2Z_0}{\pi a}} \frac{1}{a} \frac{u_i^2}{\sqrt{\beta_i}} \frac{1}{\sqrt{u_i^2 - 1}} \frac{1}{|J_1(u_i)|} \sqrt{\frac{1}{(ka)}}. \tag{130}$$

$$\eta_n = \sqrt{\frac{2Z_0}{\pi a}} \frac{1}{a} \frac{u_n}{\sqrt{\beta_n}} \frac{1}{|J_1(u_n)|} \sqrt{\frac{1}{(ka)}}. \tag{131}$$

From eqs. (123) and (126) to (131), taking into account that $J_1(u_n) = 0$, we obtain the final result

$$(\mathbf{e}_i, \delta \mathbf{h}_n) = 2 \frac{ka}{\sqrt{a\beta_i a\beta_n}} \frac{1}{\sqrt{u_i^2 - 1}} \frac{\delta a}{a}. \tag{132}$$

Note that in deriving this relation it has been assumed that δa is sufficiently small so that

$$\frac{1}{\sqrt{\beta}} \approx \frac{1}{\sqrt{\beta_n'}}.$$

If this condition is not satisfied, we should replace β_n with β_n' in eq. (132).

Of special interest is the case where e_i and e_n represent the TE_{11} mode and the TM_{11} mode, respectively. In this case $u_i = 1.8411$ and, letting $i = 1$ and $n = 2$ for these two modes, we get

$$(\mathbf{e}_1, \delta\mathbf{h}_2) = 1.2937 \frac{ka}{\sqrt{a\beta_1 a\beta_2}} \frac{\delta a}{a}. \tag{133}$$

From eqs. (115), (117), (125), and (133) we then obtain for the conversion coefficients T_2 and R_2

$$T_2 \simeq -R_2 \simeq 0.646 \frac{ka}{\sqrt{a\beta_1 a\beta_2}} \frac{\delta a}{a} \times A_1, \tag{134}$$

where $|A_1|^2$, $|T_2|^2$, and $|R_2|^2$ represent the incident power, and the powers transmitted and reflected in the TM_{11} mode. We can verify* that T_2 is smaller by a factor of 2 than the conversion coefficient given in Ref. 22, which is due to the fact that the assumptions of Ref. 22 imply

$$T_n \simeq (\mathbf{e}_1, \mathbf{h}_n'), \tag{135}$$

rather than eq. (117).

Note that for $\beta_2 \to 0$, we have $a\beta_2' \to u_2\sqrt{\delta a/a}$, and therefore

$$T_2 \simeq 0.646 \sqrt{\frac{u_2}{a\beta_1}} \left(\frac{\delta a}{a}\right)^{3/4}. \tag{136}$$

Note T_2 remains finite even when the TM_{11} mode approaches cutoff in the first guide.

VII. MDDE CONVERSION IN A NONUNIFDRM WAVEGUIDE

Typically, a corrugated feed is made of one or more sections of nonuniform waveguide whose surface reactance and radius are functions of z. Since a nonuniform waveguide does not in general possess a natural mode of propagation, an incident mode will be scattered in forward and backward modes. This is true even for a conical waveguide of constant surface reactance (except when $y = 0$ or $y = \infty$). The analysis of Sections V and VI gives the differential scattering parameters which allow the local coupling into forward and backward modes to be determined at any point in a uniform waveguide. We can thus obtain a set of differential equations, whose coefficients are given by the above scattering parameters, and which can be solved, at least in principle, for the mode am-

* In Refs. 22 and 23, the TM_{11} mode was cut off to the left of the junction, and for this reason there is poor agreement between those measurements and eq. (134), which is not applicable in this case. However, numerical calculations by Masterman and Clarricoats agre well with eq. (134) at frequencies well above the cutoff frequency of the TM_{11} mode, as we may verify from Fig. 11 of Ref. 24.

plitudes. We confine ourselves to a first-order treatment assuming the total scattered power is much less than the incident power, since this is the most interesting case if the feed is well designed. It is convenient to assume for the moment that only y varies with z, in which case the waveguide can be approximated by a succession of junctions of the type considered in Section V. Let the HE_{11} mode be incident at the input ($z = z_1$). We wish to determine the resulting amplitude $T_2(z)$ of the HE'_{11} mode for $z = z_2$. If the variation of y is sufficiently slow, we can neglect reflections and determine T_2 assuming the amplitude A_1 of the HE_{11} mode is nearly constant. The transverse field of the fundamental mode is then

$$A_1 \mathbf{e}_1 e^{-j\Phi_1(z)}, \tag{137}$$

where

$$\frac{d\Phi_1}{dz} = \beta_1. \tag{138}$$

The effect on the HE'_{11} mode of a small variation δy at $z = \xi$ is to produce at $z \gtrsim z_2$ a component

$$dT_2 = t_2(\xi)\delta y A_1 e^{-j\Phi_1(\xi)} e^{-j[\Phi_2(z_2) - \Phi_2(\xi)]}, \tag{139}$$

where

$$\frac{d\Phi_2}{dz} = \beta_2, \tag{140}$$

and from Eq. (86),

$$t_2(\xi) = \frac{-1}{a\beta_1 - a\beta_2} \sqrt{\frac{u_1 u_2}{a^2 \beta_1 \beta_2} \frac{1}{|(dy/du_1)(dy/du_2)|}}. \tag{141}$$

Note that both β_1 and β_2 are functions of z. From eq. (139), integrating from z_1 to z_2,

$$T_2(z_2) = \int_{z_1}^{z_2} dT_2 = A_1 e^{-j\Phi_2(z_2)} \times \int_{z_1}^{z_2} t_2(z) e^{+j[\phi_2(z) - \phi_1(z)]} \frac{dy}{dz} dz, \tag{142}$$

which assumes a very simple form when $ka \gg 1$, as discussed in the following section.

7.1 Conical horn with ka ≫ 1

Suppose the radius a varies linearly with z, as shown in Fig. 1 for $z > z_1$, that the flare angle α is very small, and

$$ka(z) \gg 1$$

for $z_1 < z < z_2$. It was shown in Section III that for $ka \gg 1$ the properties of a mode are entirely determined* by y/ka and, therefore, a mode will propagate without variation of its transverse field distribution if y/ka = constant. For this reason, it is reasonable to assume that mode conversion will be negligible if

$$\delta\left(\frac{y}{ka}\right) = 0. \tag{143}$$

Under this assumption, the effect on the amplitude of the HE'_{11} mode for $z = z_2$ of a small variation $\delta(y/ka)$ occurring at $z = \xi$ can be expressed in the form

$$dT_2 = \tau_2(\xi)\delta\left(\frac{y}{ka}\right) A_1 e^{-j\Phi_1(\xi)} e^{-j[\phi_2(z_2)-\phi_2(\xi)]}, \tag{144}$$

where, since eqs. (144) and (139) must agree in the particular case a = constant,

$$\tau_2(\xi) = kat_2(\xi). \tag{145}$$

From eq. (96),

$$\tau_2 = -\frac{u_1 u_2}{u_2^2 - u_i^2} \quad (ka \gg 1). \tag{146}$$

Therefore,

$$T_2(z_2) = -A_1 e^{-j\Phi_2(z_2)} \frac{u_1 u_2}{u_2^2 - u_1^2} \int_{z_1}^{z_2} e^{j[\Phi_1(\xi)-\Phi_2(\xi)]} d\left(\frac{y}{ka}\right). \tag{147}$$

Note that, since $ka \gg 1$,

$$a\beta_i \approx ka - \frac{1}{2}\frac{u_i^2}{ka}. \tag{148}$$

Therefore, from eqs. (138) and (140)

$$\frac{d}{dz}[\Phi_1(z) - \Phi_2(z)] = \frac{k}{2}\frac{u_2^2 - u_1^2}{(ka)^2}. \tag{149}$$

Now, a varies linearly with z,

$$a = (z - z_0)\tan\alpha, \tag{150}$$

* Since now we are dealing with a conical waveguide, each mode is a spherical wave centered at the apex A of the waveguide, and the field distribution over a spherical wavefront is given to a first approximation (small α) by eqs. (35) and (37). To obtain the field distribution over a plane z = constant, we must therefore introdce in eqs. (35) and (37) a factor of exp $(-j\psi)$, $\psi = k(x^2 + y^2)/2R$, R being the distance of the plane from the apex.

where z_0 is the value of z at the apex of the waveguide. Therefore, from eqs. (149) and (150)

$$\Phi_1(z) - \Phi_2(z) = -\frac{1}{2}\frac{u_2^2 - u_1^2}{\mathrm{y}\tan\alpha}\frac{\mathrm{y}}{ka}. \tag{151}$$

Of particular interest is the case

$$\mathrm{y} = \text{constant}. \tag{152}$$

Then eq. (147) can be readily integrated. Taking into account eq. (151), we obtain

$$|T_2|^2 = |A_1|^2 \frac{4u_1^2u_2^2\mathrm{y}^2\tan\alpha^2}{(u_2^2 - u_1^2)^4} \times \left|1 - \exp\left[j\frac{1}{2}\frac{u_2^2 - u_1^2}{\mathrm{y}\tan\alpha}\frac{\mathrm{y}}{ka_1}\left(1 - \frac{a_1}{a_2}\right)\right]\right|^2, \tag{153}$$

where $a_i = a(z_i)$. Therefore,

$$|T_2|^2 \leqq |A_1|^2 \frac{16u_1^2u_2^2\mathrm{y}^2\tan\alpha^2}{(u_2^2 - \mathrm{u}_1^2)^4}, \tag{154}$$

where it is recalled that $u_2 = 5.1356$ and $u_1 = 2.4048$. For $\alpha = 4°$, which is the value chosen in the experiment of Ref. 17, this inequality gives for $\mathrm{y} = 1$

$$\frac{|T_2|^2}{|A_1|^2} \leqq 0.6636\ 10^{-4}, \quad (-41.8\ \mathrm{dB}), \tag{155}$$

which is a very small value for most aplications. For $\alpha = 16°$, on the other hand, we obtain -29.8 dB, which may no be negligible.

Note that $|T_2|^2$ and $|A_1|^2$ are, respectively, the powers carried by the HE_{11}' mode and the HE_{11} mode.

VIII. SUMMARY

In the feed of Fig. 1, when a TE_{11} mode is incident at the input, some of the incident power is in general reflected. Furthermore, some power may be converted to unwanted modes if the corrugated waveguide supports more than one mode at the input. Additional mode conversion may take place inside the feed if the variation of the radius and of the surface reactance is not gradual enough. As a result, a feed will have a nonzero input reflection and, at some frequencies, unwanted modes may illuminate the aperture of the feed. The consequences of these unwanted modes on the radiation characteristics—e.g., enhanced cross polarization—are pointed out in Section III and in Ref. 17, where the theory is compared with experiment.

These effects can be evaluated to good accuracy using the expressions derived in this article, as highlighted below. For large ka, eq. (35) ex-

presses the field shape for all copolarized hybrid modes of various radial harmonics with the same ϕ dependence, while eq. (37) corresponds to the cross-polarized modes. Equation (36) gives the mode amplitudes required to normalize the power carried by the modes.

A property of corrugated feeds is that the aperture field distribution does not remain constant with frequency, as in the case of a feed with smooth walls, but varies because of the frequency dependence of the surface reactance X_s. Thus, although the desired mode has no cross-polarized component at the resonant frequency of the corrugations, at other frequencies the *desired mode does radiate* some cross polarization. The ratio, C^2, between the maximum value of the cross-polarized power in the radiation pattern and the maximum value of the copolarized power (which occurs on axis) is given by eq. (39). From eq. (39), it follows that with large ka and thin disks one can maintain low cross-polarized power in the radiation pattern from the desired mode over an octave or more.

At a junction between waveguides of the same diameter but of different surface reactance, eq. (85) gives the general expression for the mode coupling coefficient to modes reflected from the transition, and Eq. (86) gives that for modes transmitted forward from the transition. Equations (97) and (96) are simplifications of eqs. (85) and (86), respectively, which apply for $ka \gg 1$. When the input waveguide is smooth, the mode coupling coefficient is given by eq. (100) for reflected TM modes, by eq. (102) for reflected TE modes, and by eq. (103) for hybrid modes transmitted forward from the transition. Since the transition from smooth to corrugated waveguide is a major source of unwanted modes in a corrugated horn, eq. (103) is very useful in determining mode purity. Another important formula is eq. (87), which determines the reflection coefficient of the dominant mode (return loss) for any transition in X_s and any ka.

Another source of generation of undesired modes is the mode conversion occurring along the conical taper of a corrugated horn. Equation (154) gives the mode-coupling coefficient for the transmitted undesired mode due to a conical taper.

In some cases a step in diameter may be used to match transitions between different surface impedances; eq. (134) determines the mode-coupling coefficients at a step in diameter.

APPENDIX A

Asymptotic Series for u and γ in Terms of 1/ka

We determine the asymptotic series for u and γ in terms of

$$\frac{1}{ka}, \tag{156}$$

under the assumption $y \neq 0$. It is convenient to introduce in eq. (20) the quantity[12]

$$F = \frac{uJ_1'(u)}{J_1(u)} = u\frac{J_0(u)}{J_1(u)} - 1. \tag{157}$$

Note that

$$\frac{dF}{du} = \frac{J_0(u)}{J_1(u)} - u - u\frac{J_1'(u)}{J_1(u)}\frac{J_0(u)}{J_1(u)}. \tag{158}$$

But from eq. (157)

$$\frac{J_0(u)}{J_1(u)} = \frac{F}{u} + \frac{1}{u}.$$

Therefore, eq. (158) gives

$$\frac{dF}{du} = -\frac{1}{u}F^2 + \left(\frac{1}{u} - u\right). \tag{159}$$

It follows that

$$u\frac{dF}{du} + F^2 - 1 + u^2 = 0, \tag{160}$$

$$u\frac{d^2F}{du^2} + \frac{dF}{du}(1 + 2F) + 2u = 0, \tag{161}$$

$$u\frac{d^3F}{du^3} + 2\frac{d^2F}{du^2}(1 + F) + 2\left(\frac{dF}{du}\right)^2 + 2 = 0, \tag{162}$$

etc.

In terms of F, eq. (20) can be rewritten

$$yu^2\frac{1}{ka}F - F^2 + 1 - u^2\left(\frac{1}{ka}\right)^2 = 0, \tag{163}$$

or, using eq. (159),

$$yu\frac{1}{ka}F + \frac{dF}{du} + u\left[1 - \left(\frac{1}{ka}\right)^2\right] = 0. \tag{164}$$

Now assume

$$u = u_{0m}\left[1 + \alpha_1\frac{1}{ka} + \alpha_2\left(\frac{1}{ka}\right)^2 + \cdots\right]. \tag{165}$$

Develop F in a Taylor series about the point $u = u_{0m}$,

$$F = F(u_{0m}) + \left(\frac{dF}{du}\right)_{u=u_{0m}}(u - u_{0m}) + \cdots. \tag{166}$$

From eqs. (160) to (162), with $u = u_{0m}$, taking into account that

$$F(u_{0m}) = -1, \tag{167}$$

we obtain for the derivatives appearing in eq. (166),

$$\left.\begin{aligned} \left(\frac{dF}{du}\right)_{u=u_{0m}} &= -u_{0m} \\ \left(\frac{d^2F}{du^2}\right)_{u=u_{0m}} &= -3. \\ \left(\frac{d^3F}{du^3}\right)_{u=u_{0m}} &= -2\frac{1+u_{0m}^2}{u_{0m}}, \text{ etc.} \end{aligned}\right\} \tag{168}$$

Substituting eqs. (165), (167), and (168) in eq. (166) one obtains F as a series of powers of $1/ka$; the coefficients of this series are algebraic expressions in u_{0m} and α_1, α_2, etc. Similarly, by developing dF/du in a Taylor series about the point $u = u_{0m}$, and then using eqs. (165), (167), and (168), we obtain dF/du as a series of powers of $1/ka$. Substituting eq. (165) and the above series expansions of F and dF/du in eq. (164), we can solve for the coefficients α_1, α_2, etc. We obtain eq. (31). Substituting eq. (31) in eq. (166) we obtain an expansion of F in powers of $1/ka$. Using these results, from

$$\gamma = -\frac{F}{\cos\theta_1} = -\frac{F,}{\sqrt{1-\left(\frac{u}{ka}\right)^2}}, \tag{169}$$

we get eq. (32).

Equations (31) and (32) have been obtained assuming eq. (165), which corresponds to the limiting case of eq. (28). If, instead of assuming eq. (165), we assume

$$u = u'_m = u_{2m}\left[1 + \beta_1\left(\frac{1}{ka}\right) + \beta_2\left(\frac{1}{ka}\right)^2 + \cdots\right], \tag{170}$$

we obtain eqs. (33) and (34).

APPENDIX B

Surface Wave Mode

In addition to the modes considered in Section III, there is a mode for which $\beta > k$. Thus, since for this mode $\cos\theta_1 > 1$, it is convenient to replace θ_1 with $j\theta_1$ in eqs. (16) and (18). Since

$$\left.\begin{aligned} \cos j\theta &= \cosh\theta_1 \\ \sin j\theta_1 &= j\sinh\theta_1 \\ J_1(jx) &= jI_1(x), \\ J'_1(jx) &= I'_1(x), \end{aligned}\right\}, \tag{171}$$

where $I_1(x)$ is the modified Bessel function of order 1, we obtain from eqs. (16) and (17)

$$\gamma = -\frac{I_1'(u)}{I_1(u)}\frac{u}{\cosh \theta_1}, \tag{172}$$

$$\frac{\mathrm{y}}{ka} = -\left[\frac{1}{u}\frac{I_1'(u)}{I_1(u)} + \frac{\cosh \theta_1}{u}\frac{1}{\gamma}\frac{1}{u}\right], \tag{173}$$

where $u = ka \sinh \theta_1$. We can verify from these two equations that $u \to \infty$ as $ka \to \infty$. Now, for large u,

$$I_1'(u) \approx I_1(u) \approx \frac{e^u}{\sqrt{2\pi u}}. \tag{174}$$

Therefore eq. (172) gives

$$\gamma \to \infty, \quad \text{as } ka \to \infty.$$

From eq. (173), for large u and ka,

$$\frac{\mathrm{y}}{ka} \approx -\frac{1}{u}. \tag{175}$$

Therefore, since $u = ka \sinh \theta_1$,

$$\sinh \theta_1 \approx -\frac{1}{\mathrm{y}}. \tag{176}$$

We now examine the behavior of the field components for $ka \to \infty$. Taking into account eq. (171), from eqs. (10) to (15), after replacing θ_1 with $j\theta_1$, we find for $\gamma = -\infty$ (i.e., for $B = 0$) that the only nonzero component of the magnetic field is H_ϕ and

$$-Z_0 H_\phi = \frac{1}{\sinh \theta_1} A I_1'\left(u\frac{r}{a}\right) \cos\phi\, e^{-j\beta z}.$$

Therefore, for $kr \gg \mathrm{y}$

$$-Z_0 H_\phi \approx A' \sqrt{\frac{a}{r}} \cos\phi \exp[k(r-a)\sinh \theta_1 - j\beta z],$$

where A' is a constant. This shows that the field is confined to the near vicinity of the wall, decaying approximately exponentially from the wall.

We can show that $ka > 1.81$, the surface wave mode in combination with the $\mathrm{HE}_{1\mathrm{m}}$ and $\mathrm{HE}_{1\mathrm{m}}'$ modes comprise the complete set of propagating modes whose E_z azimuthal dependence is $\cos\phi$.

APPENDIX C

Derivation of dy/du

From eq. (163),

$$\frac{y}{ka} = \frac{1}{u^2}F + \left(\frac{1}{(ka)^2} - \frac{1}{u^2}\right)\frac{1}{F}.$$

where

$$F = \frac{uJ_1'(u)}{J_1(u)}.$$

Furthermore, from eq. (164)

$$F' = -\frac{1}{u}F^2 + \left(\frac{1}{u} - u\right).$$

Therefore,

$$\frac{1}{ka}\frac{dy}{du} = -\frac{2}{u^3}\left(F - \frac{1}{F}\right) + \frac{1}{u}\left[\left(\frac{1}{ka}\right)^2 - 1\right] - \frac{1}{u^3}F^2 - \left(\frac{1}{u} - u\right)\left[\left(\frac{1}{ka}\right)^2 - \frac{1}{u^2}\right]\frac{1}{F^2}. \quad (178)$$

For the case $y \to \infty$, we now determine

$$\lim_{y\to\infty}\frac{dy}{du}.$$

For $y \eqsim \infty$ there are two types of modes: TE modes, in which case $\gamma \eqsim 0$, and TM modes, in which case $\gamma \eqsim \infty$. In the former case from eq. (169) we have $F \eqsim 0$ and, therefore, eq. (178) gives

$$\lim_{y\to\infty}\frac{dy}{du} = -\frac{1}{u}(u^2 - 1)\frac{(ka)^2 - u^2}{u^2 ka}\frac{1}{F^2} = -y^2(u^2 - 1)\frac{kau}{(ka)^2 - u^2}, \quad (\gamma \eqsim 0) \quad (179)$$

since from eq. (163) for $F \eqsim 0$

$$\lim_{y\to\infty} F = -\frac{1}{y}\frac{(ka)^2 - u^2}{kau^2}$$

In the latter case ($\gamma \eqsim \infty$) from eq. (169), we have $F \eqsim \infty$. More precisely, from eq. (163)

$$F \eqsim \frac{u^2}{ka}y,$$

and therefore from eq. (178)

$$\frac{dy}{du} \eqsim \frac{ka}{u^3}F^2 \eqsim -\frac{u}{ka}y^2 \quad (\gamma \eqsim \infty). \quad (180)$$

APPENDIX D

Cutoff Frequencies of the Modes of Equations (35) and (37)

From eqs. (16) and (17) we get

$$\gamma^2 + \gamma\omega - 1 = 0,$$

where

$$\omega = \frac{yu^2}{ka\cos\theta_1}.$$

Therefore, either

$$\gamma = \frac{-\omega + \sqrt{\omega^2 + 4}}{2} \tag{181}$$

or

$$\gamma = \frac{-\omega - \sqrt{\omega^2 + 4}}{2}, \tag{182}$$

respectively, in the two cases of eqs. (35) and (37) (which correspond, respectively, to $\gamma \to 1$ and $\gamma \to -1$ for $ka \to \infty$). At cutoff $\beta \to 0$; i.e., $\cos\theta_1 \to 0$. For $\cos\theta_1 \simeq 0$, $y \neq 0$, we have $|\omega| \to \infty$ and, therefore, from eq. (181)

$$\gamma \to \begin{cases} 0 & \text{if } y > 0 \\ \infty & \text{if } y < 0 \end{cases}, \tag{183}$$

(184)

whereas from eq. (182)

$$-\gamma \to \begin{cases} \infty, & \text{if } y > 0 \\ 0, & \text{if } y < 0 \end{cases}.$$

If $\gamma = 0$, the mode is of the TE type. Now, for a TE mode at cutoff, the only nonzero component of the magnetic field is H_z and therefore the surface reactance X_s has no effect on the cutoff frequency. This means that the cutoff frequency can be determined by replacing the corrugated wall with a smooth wall of radius a, and therefore the cutoff frequency is determined by the condition:

$$J_1'(ka) = 0.$$

If $\gamma = \infty$, on the other hand, the mode is of the TM type and the only nonzero component of the electric field at cutoff is E_z. It follows that if the disks are very thin ($t \simeq 0$), they can be removed without affecting the field. Thus, the cutoff frequency can in this case be determined by replacing the corrugated waveguide with a smooth waveguide of radius b. It is thus determined by the condition

$$J_1(kb) = 0.$$

When y = 0, $\gamma = \pm 1$, and from eq. (16), $J_1'(ka) = 0$ for $\cos\theta_1 = 0$. Thus, when y = 0 both types of mode have the same cutoff frequencies.

REFERENCES

1. A. F. Kay, "The Scalar Feed," U.S. Air Force, Cambridge Research Laboratory Report, 62-347, March 1964.
2. V. H. Rumsey, "Horn Antennas with Uniform Power Patterns Around Their Axes," IEEE Trans. Ant. Propag., *AP-14*, No. 5 (September 1966), pp. 656–658.
3. A. F. Kay, "A Wide Flare Horn—A Novel Feed for Low Noise Broadband with High Aperture Efficiency Antennas," U.S. Air Force, Cambridge Research Laboratory Report, 62-757, October 1962.
4. H. C. Minnett and B. MacA. Thomas, "A Method of Synthesising Radiation Patterns with Axial Symmetry," IEEE Trans. Ant. Propag., *AP-14*, No. 5 (September 1966), pp. 654–656.
5. T. S. Chu, unpublished work, 1967.
6. H. C. Minnett and B. MacA. Thomas, "Fields in the Image Space of Symmetrical Focusing Reflectors," Proc. IEE, *115*, No. 10 (October 1968), pp. 1419–1430.
7. G. H. Bryant, "Propagation in Corrugated Waveguides," Proc. IEE, *116*, No. 2 (February 1969), pp. 203–213.
8. B. MacA. Thomas, "Bandwidth Properties of Corrugated Conical Horns," Electron. Lett., *5*, No. 22 (October 30, 1969), pp. 561–563.
9. M. S. Narasimlion and B. V. Rao, "Hybrid Modes in Corrugated Conical Horns," Electron. Lett., *6*, No. 2 (January 22, 1970), pp. 32–34.
10. T. B. Vu and Q. H. Vu, "Optimum Feed for Large Radio Telescopes: Experimental Results," Electron. Lett., *6* (March 19, 1970), pp. 159–160.
11. B. MacA. Thomas, "Prime-Focus One- and Two-Hybrid-Mode Feeds," Electron. Lett., *6*, No. 15 (July 1970), pp. 460–461.
12. P. J. B. Clarricoats and P. K. Saha, "Propagation and Radiation Behaviour of Corrugated Feeds; Part 1—Corrugated Waveguide Feed," Proc. IEE, *118*, No. 9 (September 1971), pp. 1167–1176.
13. P. T. B. Clarricoats and P. K. Saha, "Propagation and Radiation Behaviour of Corrugated Feeds; Part 2—Corrugated-Conical-Horn Feed," Proc. IEE, *118*, No. 9 (September 1971), pp. 1177–1186.
14. B. MacA. Thomas, "Theoretical Performance of Prime-Focus Paraboloids Using Cylindrical Hyhrid-Mode Feeds," Proc. IEE, *118*, No. 11 (November 1971), pp. 1539–1549.
15. T. B. Vu, "Low-Noise Dual-Hyhrid-Mode Horn—An Experimental Model," Int. J. Electron., *34*, No. 3 (1973), pp. 391–400.
16. M. Mizusawa, F. Takeda, and S. Betsudau, "Radiation Characteristics of a Corrugated Conical Horn," Electron. Commun. Jap., *56-B*, No. 1 (January 1973), pp. 42–47.
17. C. Dragone, "Characteristics of a Broadband Corrugated Feed: A Comparison Between Theory and Experiment," this issue, pp. 869–888.
18. J. Brown, "Electromagnetic Momentum Associated with Waveguide Modes," Proc. IEE, *113*, No. 1 (January 1966), pp. 27–34.
19. L. Lewin, *Theory of Waveguides*, New York: John Wiley, 1955.
20. R. E. Collin, *Field Theory of Guided Waves*, New York: McGraw-Hill, 1960.
21. D. Marcuse, *Light Transmission Optics*, New York: Van Nostrand, 1972.
22. E. R. Nagelherg and J. Shefer, "Mode Conversion in Circular Waveguides," B.S.T.J., *44*, No. 7 (Septemher 1965), pp. 1321–1338.
23. K. K. Agarwal and E. R. Nagelherg, "Phase Characteristics of a Circularly Symmetric Dual-Mode Transducer," IEEE Trans. Microw. Theory Tech., *MTT-18*, No. 1 (January 1970), pp. 69–71.
24. P. H. Masterman and P. J. B. Clarricoats, "Computer Field-Matching Solution of Waveguide Transverse Discontinuities," Proc. IEE, *118*, No. 1 (January 1971), pp. 51–63.
25. B. MacA. Thomas, "Mode Conversion Using Circumferentially Corrugated Cylindrical Waveguide," Electron. Lett., *8*, No. 15 (July 27, 1972), pp. 394–396.